REGENERATIVE AC ELECTRONIC LOAD WITH LCL FILTER

Rafael Luís Klein, Angelo Fillipi de Paiva and Marcello Mezaroba
Núcleo de Processamento de Energia Elétrica – nPEE – Departamento de Engenharia Elétrica
Universidade do Estado de Santa Catarina UDESC – CCT
Campus Universitário Prof. Avelino Marcante s/n – Joinville/SC – Brasil
CEP 89223-100 – Phone Number +55 47 4009-7844
rafaelluisklein@gmail.com, fillipi.angelo@gmail.com, mezaroba@joinville.udesc.br

***Abstract* – This article present the design and implementation of a regenerative AC electronic load with LCL filter. The electronic load is composed by a current controlled rectifier, which drains from the equipment under test (EUT) the desired current profile, and a current controlled inverter connected to the grid, which is responsible for power regenerating. The control strategy, modeling and design of the controllers are presented. Experimental results on a prototype of 4.5 kVA are presented to validate the proposed system.**

***Keywords* - Electronic load, energy regeneration, LCL filter.**

I. INTRODUCTION

The traditional method used to perform the burn-in tests on UPS consists in the association of resistors, capacitors, inductors and static converters, trying to reproduce the desired load profile defined by the end-user or standards for the given applications. Many times, this solution results in heavy and large equipments, besides the large energy consumption during the tests. Furthermore, every time a different load configuration is required, the reconfiguration of the load bank will be required, increasing the test time and resulting in high operating costs. Thus, not only the energy tested is wasted, but also the operation is inconvenient [1].

Among the main advantages in the use of regenerative electronic load, include: reducing energy consumption, reducing the area occupied by testing devices with conventional loads, reducing installation costs and energy consumption of cooling systems, reducing of peak power demand, ease and flexibility in configuration of various types of linear and non-linear loads.

Many papers have been published in recent years on energy recyclers applied to UPS [1]-[4]. However these studies utilize the L filter, which uses an inductor for connecting the converter and the EUT. However for high power systems the inductance value tends to be too large, making the filter large and expensive, besides damaging the dynamic response of the system [5]-[6].

Alternatively the second order LC filter can be used, however when connecting to the electronic load some equipment with low output impedance, such as UPS and ac source can occur the following situations: current circulation between the high frequency converters; resonance between filters and instability of control system.

Another alternative is the use of LCL filter, which has a higher harmonic attenuation in high frequency, resulting in lower inductance values and consequently lower volume and weight [5]-[6]. However, the LCL filter has a resonance peak in its frequency spectrum, which may unsettle the feedback system. The resonance dampening LCL filter can be performed by using passive or active. The passive method increases the losses and thus reduces system performance. [7] The active damping method is based on changes in system control loops [8]-[10].

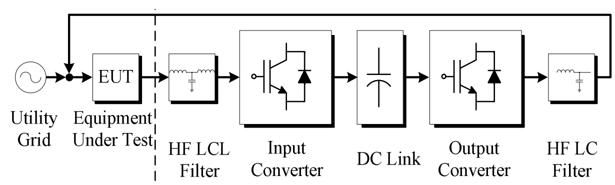

Fig. 1. Block Diagram of an equipment coupled to a regenerative electronic load.

This paper proposes the development of a regenerative AC electronic load using LCL filter with active damping through the use of a lead compensator for testing equipment such as AC Power sources, transformers, generators, UPS.

The Fig. 1 shows an application of a regenerative AC electronic load emulator.

II. PROPOSED CIRCUIT

The basic configuration of the regenerative AC electronic load with LCL filter is shown at Fig. 2. The structure is composed by two converters, both current controlled. The chosen topology for their implementation is constituted by two three-phase four wire inverters interconnected by center-tapped DC link capacitor bank, as shown at Fig. 3.

This topology, besides the harmonic compensation, also allows compensation of the unbalanced load current. It means that the emulator can operate with any type of load.

The proposed control scheme has one converter which controls the power flow of the EUT, and the other that controls the regeneration of the power to utility grid.

The input converter is connected to the EUT to drain the current according the desired load profile. The references are generated by a digital signal processor (DSP) TMS320LF2812 [11] and are synchronized with the imposed voltage by the EUT.

The output converter is connected to the utility grid and sends the drained energy back to the utility grid with unity power factor. It also regulates the DC link voltage.

The main specifications of emulator are shown in table 1.

III. CONTROL DESIGN

Fig. 4 and Fig. 5 show the block diagram of output and input converter control.

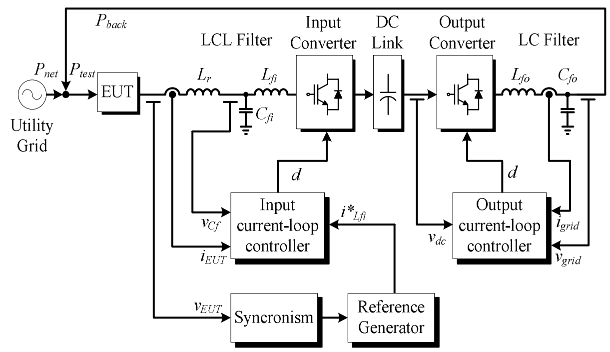

Fig. 2. Unifilar block diagram of regenerative AC electronic load.

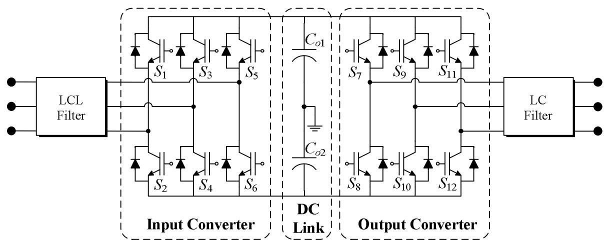

Fig. 3. Block diagram of power circuit.

TABLE I

Input and output converter specifications

$P_{3\varphi}$ = 4.5 kVA	Total output power
v_{DC} = 600 V	DC bus voltage
v_{grid} = 127 V	Phase to neutral Grid voltage
v_{EUT} = 127 V	Phase to neutral EUT voltage
Bw_i = 3 kHz	Input converter bandwidth
Bw_o = 1 kHz	Output converter bandwidth
i_{iA} - i_{iC} = i_{oA} - i_{oC} = 16 A	Input and output peak current
f_s = 50 kHz	Switching frequency

The output converter controller consist of three identical current feedback loops, one for each phase, in order to control the output current, one voltage feedback loop to control the DC link voltage and another one unbalanced-voltage feedback loop to keep the voltage on the DC link capacitor bank balanced.

The voltage control loop has a low response and determines the reference signal amplitude of current controller. The unbalanced-voltage control loop, is a DC level loop, acts on the average reference value of the current controller, in order to keep the DC link voltage balanced. The current control consists of three identical current loops, except for the 120 degrees phase shift from each other. The current loops have a fast response, allowing the decoupling of this with the voltage loop.

The input converter controller is composed by six control loops: three current and three damping. The damping loop is responsible for attenuating the resonance peak of the LCL filter. The current loop must be able to control the current drawn from the EUT as the reference imposed on the controller by a DSP synchronized with the imposed voltage by the EUT.

The current, voltage and unbalance-voltage control is designed with PI + pole compensator. This compensator provides phase lead at high frequencies, which enhances the responsiveness and stability of the system and phase lag at low frequencies which reduces the steady state error.

The damping control uses only a lead element in the reference applied to the feedback from the capacitor voltage. According to the methodology presented in [10] the lead angle, maximum frequency and gain of the lead compensator should be chosen to attenuate the resonance peak of the LCL filter.

The cut-off frequency of the voltage and unbalanced voltage control are 6 Hz and 0.6 Hz respectively, these controllers should have a low response. Otherwise the current control is a fast control and its cut-off frequency is 8 kHz. All controls have phase margin between 30º e 90º.

The output converter current loop transfer function is presented in equation (1).

$$G_{i\_out}(s) = \frac{V_b}{L_f \cdot s} \cdot \frac{H_i}{Vm} \quad (1)$$

The voltage loop transfer function to output converter is presented in equation (2).

$$G_v(s) = \frac{3 \cdot m_a}{2 \cdot C_b \cdot s} \cdot \frac{K_{mp} \cdot K_v \cdot H_{vb}}{H_i} \quad (2)$$

The unbalanced voltage loop transfer function to output converter is presented in equation (3).

$$G_{uv}(s) = \frac{3}{2 \cdot C_b \cdot s} \cdot \frac{K_{uv} \cdot H_{vb}}{H_i} \quad (3)$$

The input converter current loop transfer function is presented in equation (4).

$$G_{i\_in\_damp}(s) = \frac{-V_b}{L_f \cdot L_r \cdot C_f \cdot s^3 + (L_f + L_f) \cdot s} \cdot CLTF_{G_{v\_Cf}} \cdot H_i \quad (4)$$

The damping loop transfer function to input converter is presented in equation (5).

$$G_{v\_Cf}(s) = \frac{L_r \cdot V_b}{L_f \cdot L_r \cdot C_f \cdot s^3 + (L_f + L_f) \cdot s} \cdot \frac{H_v}{Vm} \quad (5)$$

Where:

C_b	- DC Link Capacitance
H_i	- Current Sensor Gain
H_{vb}	- Voltage Sensor Gain
K_{mp}	- Multiplier Gain
K_{uv}	- Unbalance-Voltage Control Attenuation
K_v	- Voltage Control Attenuation
L_f	- Filter inductance (converter side)
L_r	- Filter inductance (grid side)
m_a	- Modulation Ratio
V_b	- DC link voltage
Vm	- Pulse Width Modulator Gain
$CLTF_{Gv\_Cf}$	- Closed-loop transfer function of G_{v_Cf}.

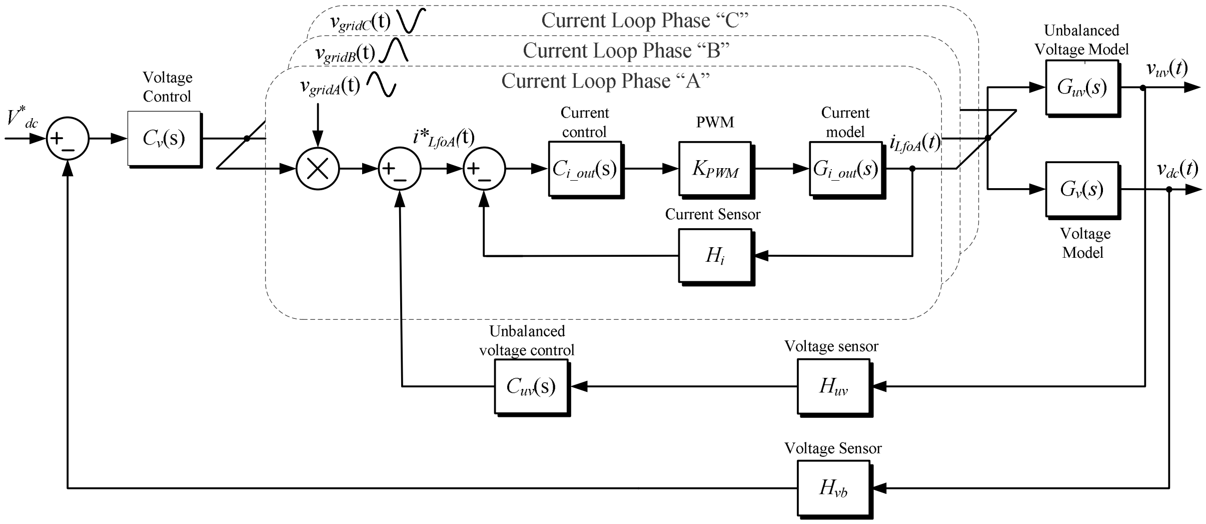

Fig. 4. Output converter control block diagram.

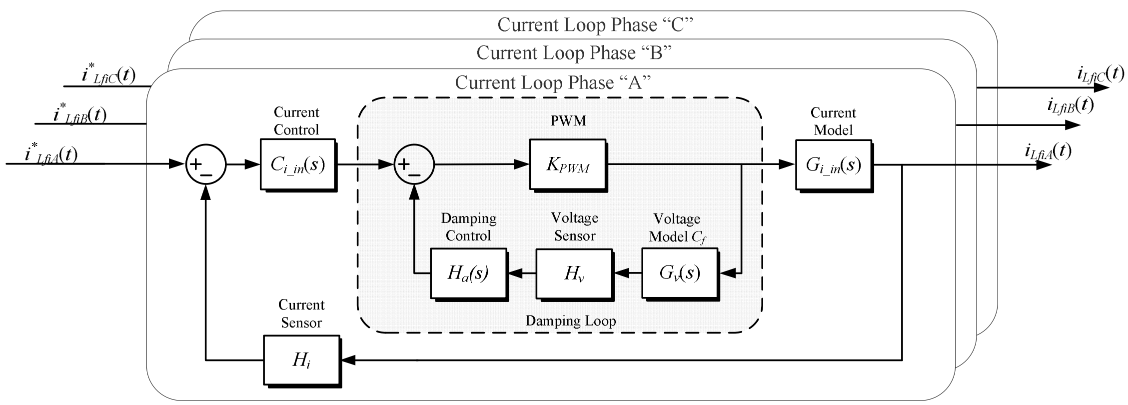

Fig. 5. Input converter control block diagram.

The proposed PI + pole compensator is shown in Fig. 6 and its transfer function is presented in equation (6).

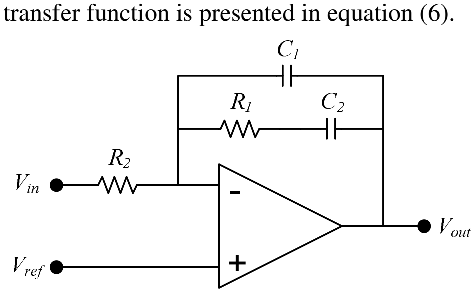

Fig.6. PI + pole compensator.

$$C(s) = \frac{(1 + s \cdot R_1 \cdot C_2)}{s \cdot R_2 \cdot (C_1 + C_2) \cdot \left(1 + \frac{s \cdot R_1 \cdot C_1 \cdot C_2}{C_1 + C_2}\right)} \quad (6)$$

The proposed lead compensator is shown in Fig. 7. Its transfer function is presented in equation (7).

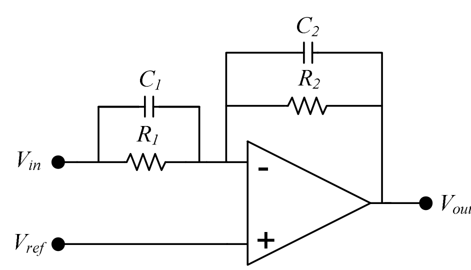

Fig.7. Lead compensator.

$$Ha(s) = \frac{R_2}{R_1} \cdot \frac{\tau s + 1}{\alpha \tau s + 1} \quad (7)$$

The current, voltage and unbalanced voltage loop frequency response of the output converter is shown in Fig. 8, Fig. 9 and Fig. 10 respectively.

The active damping and current loop frequency response of the input converter is shown in Fig. 11, Fig. 12 and Fig. 13 respectively.

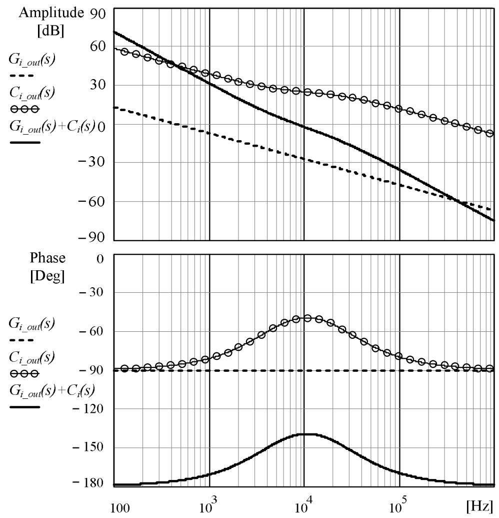

Fig. 8. Current loop frequency response of the output converter.

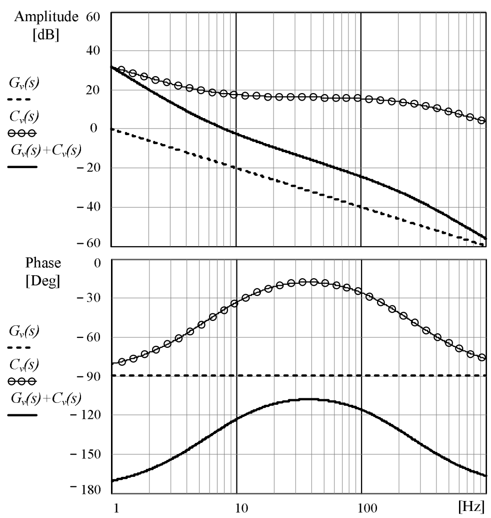

Fig. 9. Voltage loop frequency response of the output converter.

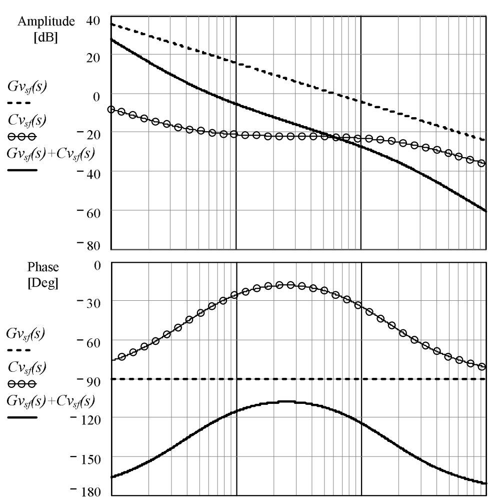

Fig. 10. Unbalanced voltage loop frequency response of the output converter.

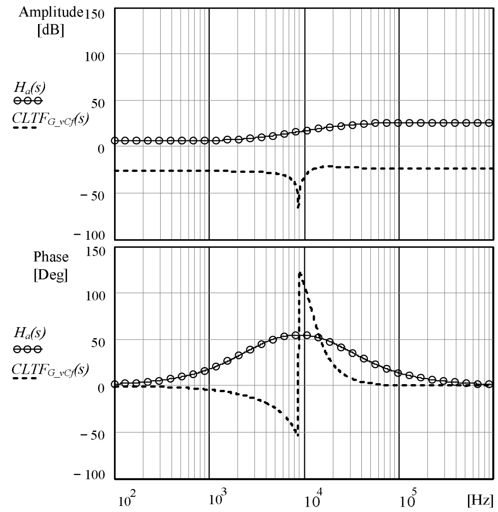

Fig. 11. Active damping loop frequency response of the output converter.

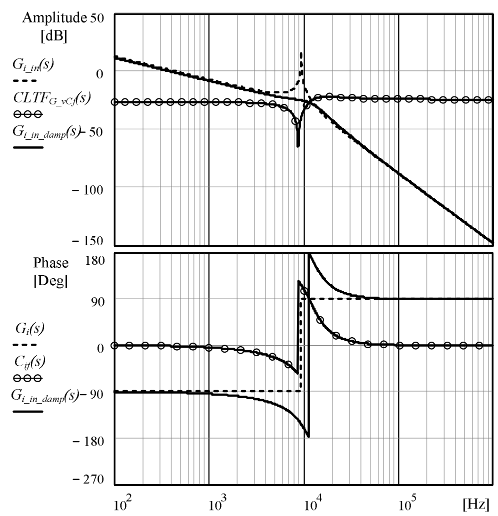

Fig. 12. Current loop frequency response of the output converter.

According to Fig. 8 the current loop with the designed controller presents phase margin equal to 40º, obeying the desired design value.

The voltage and unbalanced voltage loop with the designed controller presents phase margin equal to 43º, obeying the desired design value.

According to Fig. 11 we can observe that the closed-loop gain of the lead compensator presents a notch in the frequency it was designed to have the maximum lead angle.

Seeing that lead compensator is designed in advance to provide the maximum phase advance at exactly the resonant frequency of the LCL filter, it is noted that the notch from closed loop damping attenuates the resonance peak of the LCL filter, ie to confer damping LCL filter.

According to Fig. 13 the current loop with the designed controller presents phase margin equal to 40º, obeying the desired design value.

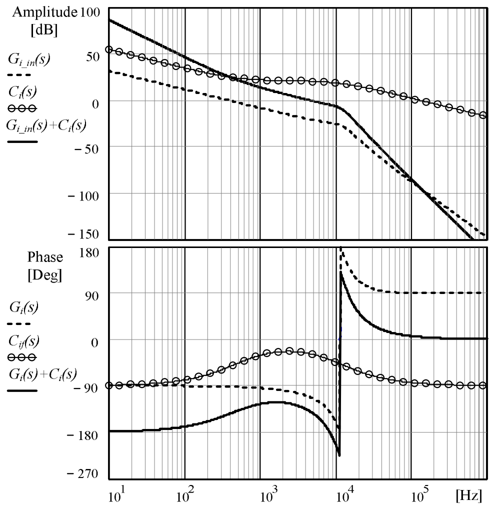

Fig. 13. Current loop frequency response of the output converter.

IV. EXPERIMENTAL RESULTS

The proposed 4.5 kVA load emulator has been implemented and tested to verify the principle of operation.

The grid voltage and frequency is selected to 127 V and 60 Hz. The EUT used was a three-phase 4.5 kVA AC power source. The prototype is shown in Fig. 14 and main prototype specifications are shown in Table 2.

Fig. 15 shows the voltage and current from EUT for the resistive load emulation. The absorbed EUT current i_{EUT} is 11 A peak, while the output converter current returned to the utility grid i_{grid} is 9 A peak. The energy loss in the input and output converter is responsible for the difference between currents i_{EUT} and i_{grid}. The overall system efficiency can reach about 80% under full-load condition when emulating a pure resistance.

TABLE II
Prototype Specifications

$S_1 – S_{12}$	Switches: IRG4PF50WD
$D_1 – D_{12}$	Switches Intrinsic Diodes
$Cb_1 – Cb_2$	Electrolytic Capacitor: 8 x 470uF/450V
$Lfi_1 – Lfi_3$, $Lfo_1 – Lfo_3$	Iron Powder Inductor: IT-560 Magmattec
$Lr_1 – Lr_3$,	Iron Powder Inductor: IT-130 Magmattec
$Cfi_1 – Cfi_3$	Polypropylene Capacitor: 3 x 1uF/630V
$Cfo_1 – Cfo_3$	Polypropylene Capacitor: 5 x 1uF/630V

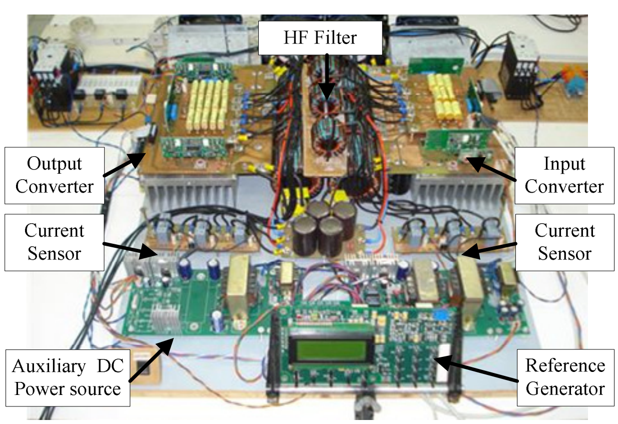

Fig. 14. Implemented prototype.

Fig. 16 shows the voltages and currents for the capacitive load emulation with 90º phase angle. The EUT current is 5 A peak, while the output converter current is practically the HF filter reactive current.

Fig. 17 shows the experimental results for three-phase currents with different load mode. The phase-A signal is composed by a nonlinear load. The phase-B signal is composed by diode bridge rectifier and phase-C is composed by resistive load.

Fig. 18 shows the voltages and currents for the resistive load emulation with EUT frequency equal to 180 Hz, while the grid frequency is equal to 60 Hz.

Fig. 19 shows the DC link voltages whose voltages are controlled in 300 V and -300 V for each of the capacitor banks.

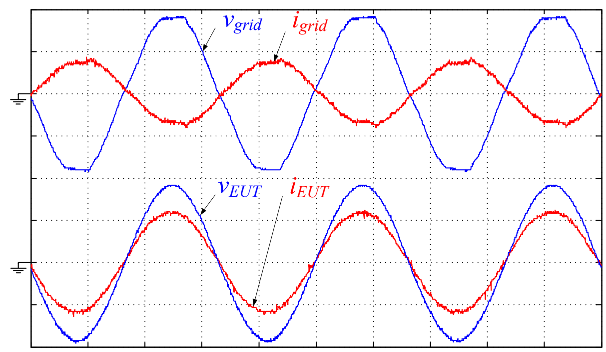

Fig. 15. Resistive Load, grid and EUT voltage (100V/div), grid and EUT current (10A/div, 5ms/div).

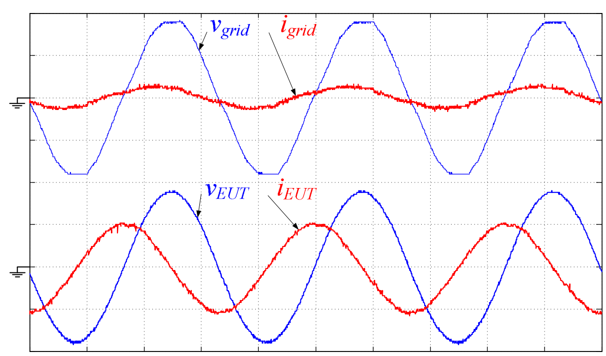

Fig. 16. Capacitive Load, grid and EUT voltage (100V/div), grid and EUT current (5A/div, 5ms/div).

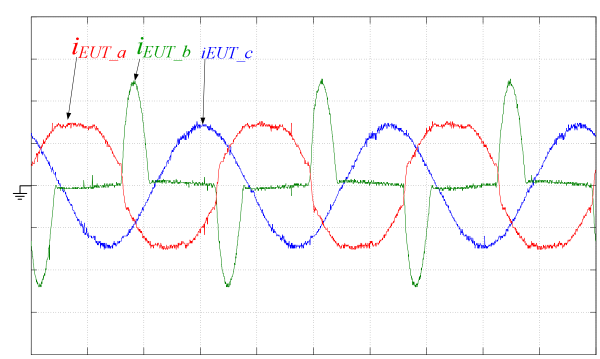

Fig. 17. Three-phase nonlinear loads, current (10A/div, 5ms/div).

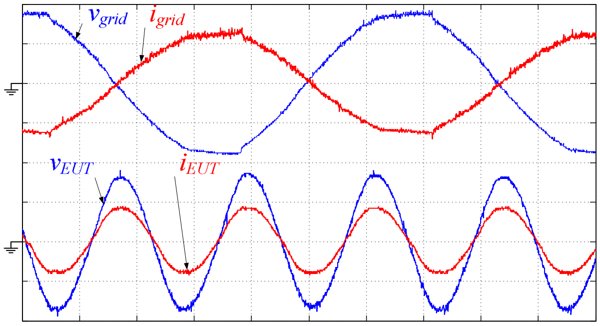

Fig. 18. Resistive Load, EUT frequency equal to 180Hz (i_{EUT}:20A/div, i_{grid}:10A/div, 100V/div, 2.5ms/div).

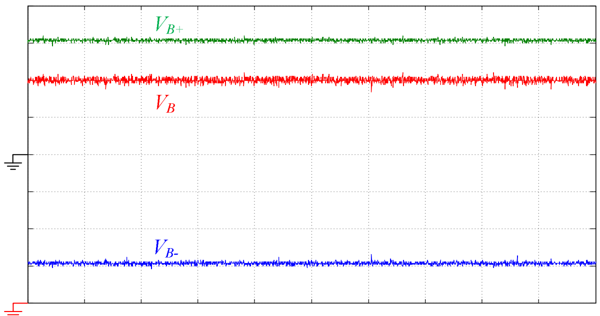

Fig. 19. DC bus voltage, (100V/div, 5ms/div).

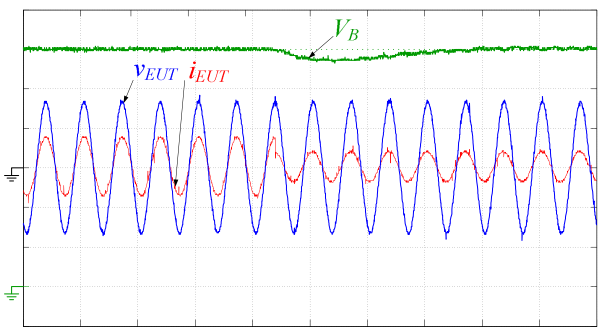

Fig. 20. Load step 100-50%, (v_{EUT}:100V/div, V_B:100V/div 20A/div, 25ms/div).

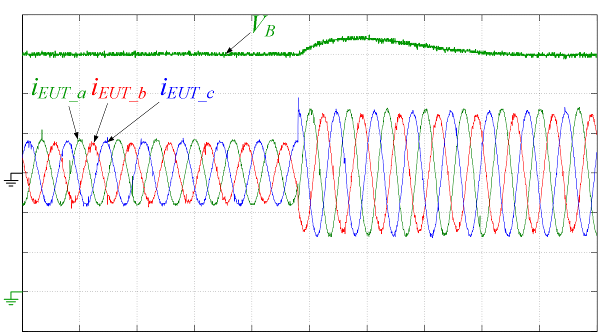

Fig. 21. Load step 50-100%, (v_{EUT}:60V/div, V_B:100V/div 10A/div, 25ms/div).

Fig. 20 and Fig. 21 shows the experimental results for a load step from 100% to 50% and 50% to 100% respectively emulating a resistive load.

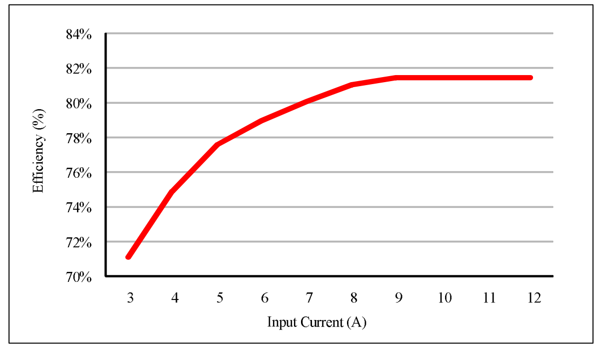

Fig. 22. Efficiency curve.

We can observe the variation of DC bus voltage and voltage compensator response to regulate de DC link, acting in output converter current.

Fig. 22 shows the shows the efficiency curve varying the current drawn from the EUT. It is observed that the maximum efficiency achieved by the structure using in the two power stages connected in series was 81.5%.

V. CONCLUSION

In this paper it was presented the applications, system architecture, operating principles, controller design and experimental results of the regenerative AC electronic load.

The proposed controllers reach all project goals and provided stable operation during all the practical tests with linear and nonlinear load emulation.

The load energy was regenerated to utility grid with unity power factor, saving a large amount of energy during the practical test.

All the waveforms in the practical tests of the proposed emulator were applied to an AC power source.

The LCL filter associated with the inductor current control on the EUT side and active damping, allowed the connection and operation of the electronic loads to the equipment with low impedance output characteristic such as AC power source.

REFERENCES

[1] S. Gupta, V. Rangaswamy, R. Ruth, “Load bank elimination for UPS testing,” in Proc. IEEE, 1990, pp. 1040–1043.

[2] C. A. Ayres and I. Barbi, “A family of converters for UPS production burn-in energy recovery,” in Proc. IEEE Transactions on Power Electronics, 1997, p. 615-622.

[3] C. L. Chu and J. F. Chen, “Self-load bank for UPS testing by circulating current method,” IEE Proc.-Electr. Power Applications, 1994, pp. 191-196.

[4] M. T. Tsai, “Comparative investigation of the energy recycler for power electronics burn-in test,” IEE Proc.-Electr. Power Applications, 2000, pp. 192-198.

[5] A. M. Julean, “Active damping of LCL filter resonance in grid connected applications,” Aalborg Universitet, Dinamarca, Dissertação de mestrado, 2009.

[6] C. Wessels, J. Dannehl, F. W. Fuchs, “Active damping of LCL-filter resonance based on virtual resistor for PWM rectifiers – Stability analysis with different filter

parameters," IEEE Power Electronics Specialists Conference (PESC), pp. 3532 – 3538, Greece, 2008.
[7] S. Wei, W. Xiaojie, D. Peng, Z. Juan, "An Over View of Damping Methods for Three-Phase PWM Rectifier," IEEE International Conference on Industrial Technology (ICIT), pp. 1 – 5, India,. 2008.
[8] M. Y. Chang, J. Y. Lin, S. L. Jung and Y. Y. Tzou, "Design and implementation of a real-time lossless dynamic electronic load simulator", IEEE Proc., 1997, pp. 734–739.
[9] S. Y. Yang, C. W. Zhabg, Z. Xie, "Study on Active Damping Methods for Voltage Source Converter with LCL Input Filter," IEEE 6th International Power Electronics and Motion Control Conference, p. 975-979, 2009.
[10] V. Blasko, V. Kaura, "A Novel Control to Actively Damp Resonance in Input LC Filter of a Three-Phase Voltage Source Converter," IEEE Transaction. on Industry Application, vol. 33, no. 2, pp. 542-550, 1997.
[11] J. A. Heerdt, N. Giacomini, J. D. Sperb, M. Mezaroba, A. L. Batschauer, "Generic generator of three-phase periodic signals for application in AC power sources." COBEP Power Electronics Conference. Blumenau, 2007.
[12] J. L. Dantas, "Reciclador de energia para testes de burn-in em fontes cc para telecomunicações", Master Thesis, Federal University of Ceará, 2006.
[13] C. A. Ayres, I. Barbi, "Power recycler for DC power supplies burn-in test: Designand experimentation", In: APEC`96 – Applied Power Electronics Conference andExposition, p. 72-78, 1996
[14] C. Zimmermann Jr., "Regenerador de energia com elevado fator de potência para o teste de burn-in de reatores eletrônicos de 250W", Master Thesis, University of Santa Catarina, 2004.
[15] M. Y. Change, J. Y. Lin, S. L. Jung, Y. Y. Tzou, "Design and implementation of a real-time lossless dynamic electronic load simulator", IEEE Proc, pp734-739, 1997.
[16] C. Wang, Y. Zou, K. Jia, F. Li, Y. Zhang, X. She, "Research onthe Power Electronic Load Based on Repetitive Controller", IEEE Proc., 2008.
[17] Y. Srinivasa Rao; Mukul Chandorkar, "Electrical Load Emulation using Power Electronic Converters", TENCON, 2008.
[18] Y. Zhou, Lei Wang, Xin Chen, "Research on Digital Controlled Converter for AC Power Electronics Burn-In Test with Energy Feedback", ICEMS, 2008.
[19] X. She, Y. She, C. Z. Wang; Y. P. Zou, "AC Electronic Load and its application in power system simulation", IEEE Proc., 2008.
[20] J. W. Baek, M. H. Ryoo, J. H. Kim; J. S. Lai, "50kVA Regenerative Active load for power test system", PEC 2007.
[21] J. Zhao, S. Pan, X. Wang, "High power energy feedback AC electronic load and its application in power system dynamic physical simulation", IEEE Proc., 2007.
[22] M-T. Tsai; C. Tsai, "Energy Recycling for Electrical AC Power Source Burn-In Test", IEEE Proc., 2000.
[23] M. T. Tsai; T. J. Cheng; C. Tsai, "High-Efficiency Energy Recycling System for AC Power Source Burn-In Test", PEDS 1999.